

The ultraviolet Sun

B. N. Dwivedi

Department of Applied Physics, Institute of Technology, Banaras Hindu University, Varanasi-221005, India

Abstract. High-resolution ultraviolet observations of the Sun from SOHO and TRACE spacecraft have provided a wealth of new information on plasma temperature, density, abundance anomaly, plasma flows, turbulence, wave motions, etc., in various solar structures. We briefly present solar physics research of our group, and review some of the new results from the SUMER spectrograph on the SOHO spacecraft, especially the widths of vacuum ultraviolet spectral lines in the equatorial solar corona observed with CDS and SUMER.

Index Terms. Solar atmosphere, ultraviolet emission, wave activity, X-ray.

1. Introduction

The discovery of the ultraviolet Sun dates back to 1801 with J.W. Ritter's observation of the decomposition of silver chloride on the short-wavelength side of the Sun's visible spectrum. However, the first clues to the hot solar atmosphere emerged from the 1869 eclipse observation of 530.3 nm green line by C.A. Young and W. Harkness. The clinching argument was the discovery by Edlén (1943) that the 'green' coronal line was in fact due to iron with 13 of its electrons stripped off. Such a situation was only possible if the plasma environment was million-degree kelvins. The 'green' and 'red' coronal lines are forbidden lines in the spectra of Fe XIV and Fe X respectively. The ultraviolet emission, that the corona is hot enough to produce, was first detected on 10 October 1946 with instruments built by R. Tousey and his colleagues at the U.S. Naval Research Laboratory using captured German military V2 rockets (Baum, Johnson, Oberly, Rockwood, Strain and Tousey, 1946). The X-ray Sun was first discovered by T.R. Burnight in 1949 using a pinhole camera on board a rocket. Since then, there has been a tremendous progress in the ultraviolet and X-ray observations from the solar atmosphere and underlying physical processes. A general article on our ultraviolet Sun has recently been written by Dwivedi (2006).

Spacecraft, built by the U.S. and Soviet space agencies in the 1960's and 1970's, dedicated to solar observations, added much to our knowledge of the Sun's atmosphere, notably the manned NASA Skylab mission of 1973-1974. Ultraviolet and X-ray telescopes onboard gave the first high-resolution images of the chromosphere and corona and the intermediate transition region. Images of active regions revealed a complex of loops which varied greatly over their lifetimes, while ultraviolet images of the quiet Sun showed that the transition region and chromosphere followed the 'network' character previously known from the Ca II K-line images. More recently, the spatial resolution of spacecraft instruments

has steadily improved, nearly equal to what can be achieved with ground-based solar telescopes (Dwivedi and Phillips, 2003). Each major solar spacecraft since Skylab has offered a distinct improvement in resolution. Fig.1 illustrates the chromosphere in the emission line of neutral helium at 58.43 nm formed at about 20,000° K. For comprehensive reviews on topics from the Sun's interior to its exterior, including the solar wind and the solar observing facilities, the reader is referred to Dwivedi (2003).

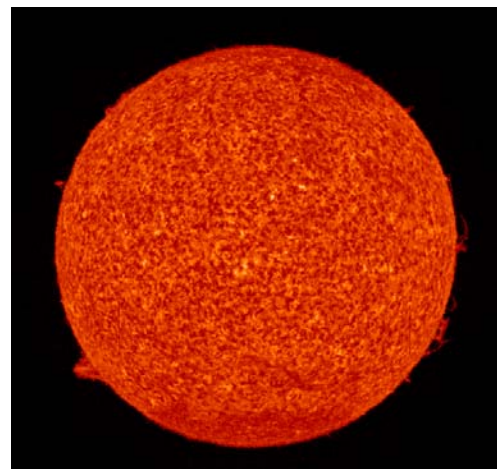


Fig. 1. The Sun's image in the chromospheric emission line of neutral helium at 58.43 nm wavelength taken by the SUMER spectrograph on the SOHO spacecraft on 4 March 1996. (Credit : SUMER/SOHO).

The ESA/NASA Solar and Heliospheric Observatory (SOHO) was launched on December 2, 1995 into an orbit about the inner Lagrangian (L1) point situated some 1.5×10^6 km from the Earth on the sunward side. Its twelve instruments, therefore, get an uninterrupted view of the Sun (Dwivedi and Mohan, 1997). There are several imaging instruments, sensitive from visible-light wavelengths to the extreme-ultraviolet. The EIT, for instance, uses normal

incidence optics to get full-Sun images several times a day in the wavelengths of lines emitted by the coronal ions Fe IX, Fe X, Fe XII, Fe XV (emitted in the temperature range 6×10^5 to 2.5×10^6 K) as well as the chromospheric He II 30.4 nm line. The CDS and the SUMER are two spectrometers operating in the extreme-ultraviolet region, capable of getting temperatures, densities and other information from spectral line ratios. The UVCS has been making spectroscopic observations of the extended corona from 1.25 to 10 solar radii from the Sun's center, determining empirical values for densities, velocity distributions and outflow velocities of hydrogen, electrons, and several minor ions.

The Transition Region and Coronal Explorer (TRACE) satellite went into a polar orbit around Earth in 1998. The spatial resolution is of order $1''$ (725 km), and there are wavelength bands covering the Fe IX, Fe XII, and Fe XV lines as well as the Ly-alpha line at 121.6 nm. Its ultraviolet telescope has obtained images containing a tremendous amount of small and varying features, for instance, active region loops are revealed to be only a few hundred kilometers wide, almost thread-like compared with their huge lengths. Their constant flickering and jouncing hint at the corona's heating mechanism. There is a clear relation of these loops and the larger arches of the general corona to the magnetic field measured in the photospheric layer. The crucial role of this magnetic field has only been realized in the past decade. The fields dictate the transport of energy between the surface of the Sun and the corona. The loops, arches and holes appear to trace out the Sun's magnetic field (cf., Figs. 2a, b). The latest in the fleet of spacecraft dedicated to viewing the Sun is the Reuven Ramaty High Energy Solar Spectroscopic Imager (RHESSI), launched in 2002, which is providing images and spectra in hard X-rays (wavelengths less than about 4 nm). RHESSI's observations of tiny microflares may provide clues to the coronal heating mechanism.

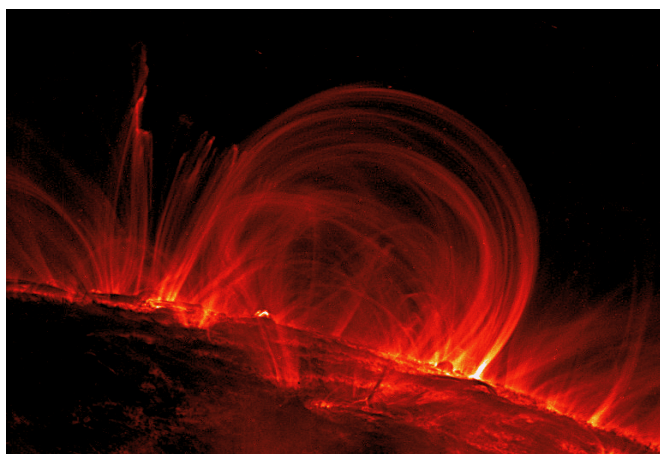


Fig. 2a. Coronal loops, observed in the ultraviolet radiation Fe IX 17.1 nm (171 Å) by the TRACE spacecraft on 6 November 1999, extending 120 000 km off the Sun's surface. (Credit: TRACE/NASA).

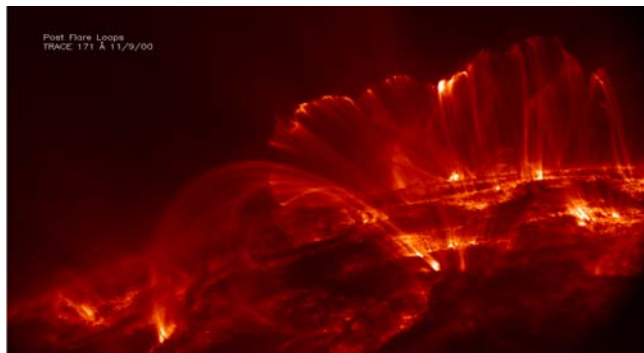


Fig. 2b. Post flare loops, observed in the ultraviolet radiation Fe IX 17.1 nm (171 Å) by the TRACE spacecraft on 9 November 2000. (Credit: TRACE/NASA).

The SUMER Spectrograph: The Sun's extreme-ultraviolet (EUV) and UV spectra, in the wavelength range from 46.5 nm to 161.0 nm (465 Å to 1610 Å) which is the spectral range of the SUMER spectrograph, provide unique opportunities for probing the solar atmosphere from the chromosphere to the corona (cf., Fig. 3).

Emission line intensities and their ratios and line shapes are used to obtain diagnostic information on plasmas in the temperature range from 10^4 K to more than 10^6 K, such as temperature, density, abundance, turbulence, and flows. A full description of SUMER spectrograph and its performance are available (Wilhelm, Curdt, Marsch et al., 1995; Wilhelm, Lemaire, Curdt et al., 1997; Lemaire, Wilhelm, Curdt et al., 1997; Wilhelm, Dwivedi, Marsch and Feldman, 2004). Briefly, the instrument is an ultraviolet telescope and spectrometer with a wavelength resolution element of $42 \text{ mÅ} - 44 \text{ mÅ}$ over the range 80.0 nm – 161.0 nm (800 Å – 1610 Å) (in first order). Along the north-south directed slit, the spatial resolution is close to $1''$ (≈ 715 km on the Sun). The spectral resolution, which is twice as high in second order, can further be improved for relative (and under certain conditions, for absolute) measurements to fractions of a pixel, allowing the measurement of Doppler shifts corresponding to plasma bulk velocities of about 1 km s^{-1} along the line of sight. There now exist a vast literature in the last ten years or so on the results from SUMER observations. Obviously, we cannot review this literature in this article. Instead, we present some significant results from SUMER on solar plasmas that have added new dimensions to a better understanding of the solar mysteries, especially coronal heating and the solar wind acceleration.

We can directly measure physical parameters such as electron density, temperature, flow speeds, etc. in the corona from emission line diagnostics. However, we cannot directly measure coronal magnetic field strength, resistivity, viscosity, turbulence, waves, etc. New powerful tools of coronal seismology have enabled the detection of MHD waves by TRACE and EIT, spectroscopic measurements of line-widths by SUMER and CDS, ion and electron temperature anisotropy measurements with UVCS, and microflares by RHESSI.

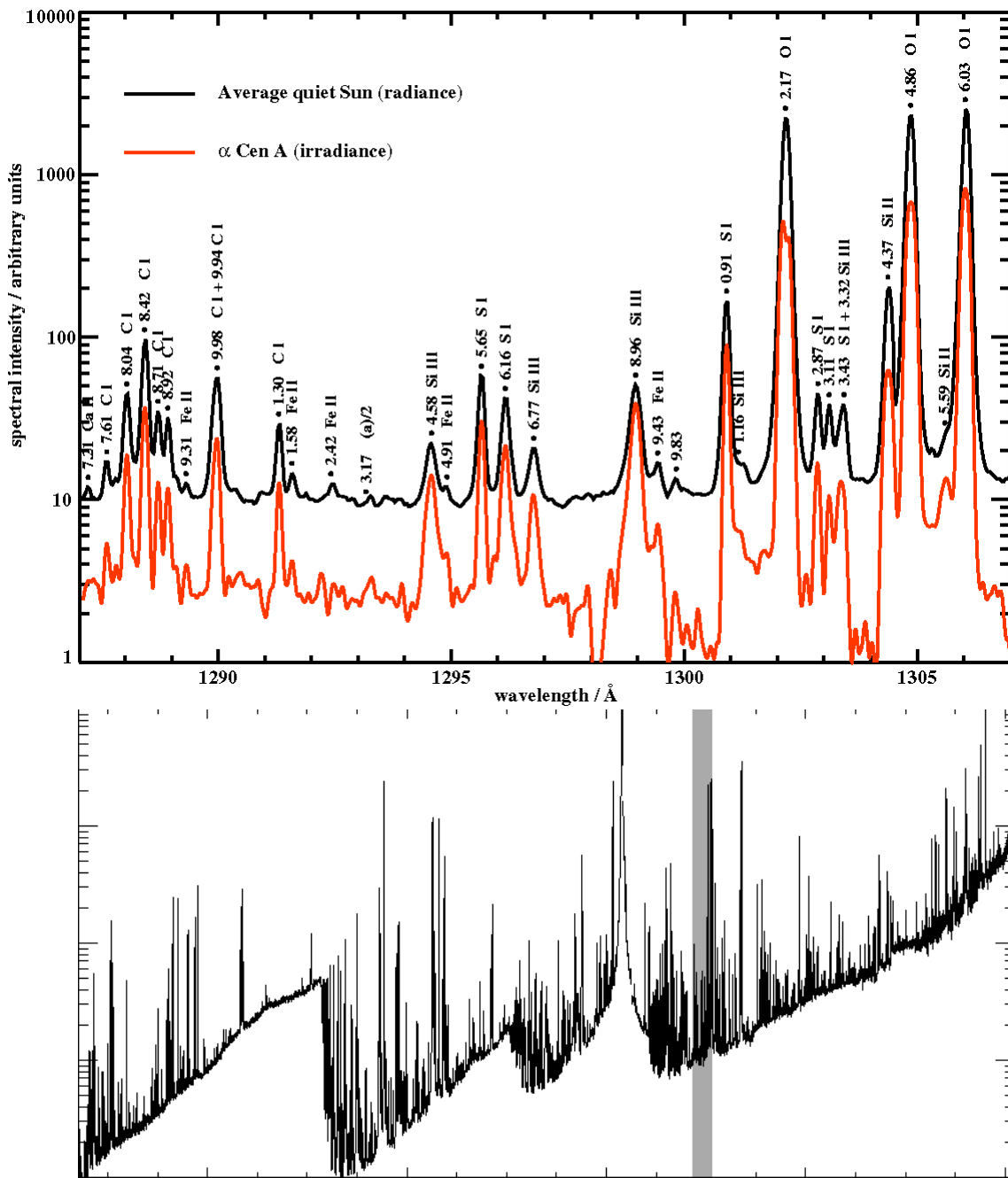


Fig. 3. Top: A close-up of a tiny part of the spectral atlas released from the SUMER instrument, compared with the irradiance spectrum of Alpha Cen A from HST-STIS. Bottom: The full extent of the spectral atlas, with the portion shown in the top panel on a shaded background. With the release of a new "spectral atlas" from the SUMER instrument on board SOHO, the world's astronomers have a much more complete roadmap of what could be described as the "Solar genome". Also likened with its "fingerprint", a star's full spectrum uniquely pins down all its defining characteristics: mass, elemental composition, age, and rotational speed. The SUMER spectral atlas is the best-ever analysis of the ultraviolet light from the Sun, spanning wavelengths from 67.0 nm to 160.9 nm (670 Å to 1609 Å), and identifies some 1100 distinct emission lines, of which more than 150 had not been recorded or identified before SOHO. (Credit: SUMER/SOHO, ESA-NASA; HST-STIS, NASA-ESA; Curdt et al., 2001).

2. Density – temperature structure, abundance anomaly

Without a knowledge of the densities, temperatures and elemental abundances of space plasmas, almost nothing can be said regarding the generation and transport of mass, momentum and energy. Thus, since early in the era of spaceborne spectroscopy we have faced the task of inferring plasma temperatures, densities and elemental abundances for

hot solar and other astrophysical plasmas from optically thin emission-line spectra (Dwivedi, 1994; Mason and Monsignori-Fossi, 1994; Dwivedi, Mohan and Wilhelm 2003; Wilhelm, Dwivedi, Marsch and Feldman, 2004, 2006). A fundamental property of hot solar plasmas is their inhomogeneity. The emergent intensities of emission lines from optically thin plasmas are determined by integrals along the line of sight (LOS) through the plasma. Spectroscopic

diagnostics of the temperature and density structures of hot optically thin plasmas using emission-line intensities is usually described in two ways. The simplest approach, the line-ratio diagnostics, uses an observed line intensity ratio to determine density or temperature from theoretical density or temperature-sensitive line-ratio curves, based on an atomic model and taking account of physical processes for the line formation. The line-ratio method is stable, leading to well-defined values of Ne or Te, but in realistic cases of inhomogeneous plasmas, these are hard to interpret, since each line pair yields a different value of density or temperature. The more general differential emission measure (DEM) method recognizes that observed plasmas are better described by distributions of temperature or density along the LOS, and poses the problem in inverse form. It is well known that the DEM function is the solution to the inverse problem, which is function of Ne or Te or both. Derivation of DEM functions, while more generally acceptable, is unstable to noise and errors in spectral and atomic data. The exact relationship between the two approaches has been investigated (Brown, Dwivedi, Almeaky and Sweet, 1991; McIntosh, Brown and Judge, 1998). Prior to the SOHO mission, there was very little information available on the density and temperature structure in coronal holes. Data from Skylab was limited, due to the very low intensities in holes

and poor spectral resolution, leading to many line blends. High-resolution ultraviolet observations from instruments on SOHO spacecraft provided the opportunity to infer the density and temperature profile in coronal holes (cf., Fig. 4a, Wilhelm, Marsch, Dwivedi et al., 1998). Comparing the electron temperatures with ion temperatures, it was concluded that ions are extremely hot and the electrons are relatively cool. Using the CDS and SUMER instruments on the SOHO spacecraft, electron temperatures were measured as a function of height above the limb in a coronal hole. Observations of two lines from the same ion, O VI 103.2 nm (1032 Å) from SUMER and O VI 17.3 nm (173 Å) from CDS, were made to determine temperature gradient in a coronal hole (David, Gabriel, Bely-Dubau, Fludra, Lemaire and Wilhelm, 1998). This way temperature of around 0.8 MK close to the limb was deduced, rising to a maximum of less than 1 MK at 1.15 R_{\odot} , then falling to around 0.4 MK at 1.3 R_{\odot} (cf., Fig. 4b). These observations preclude the existence of temperatures much over 1 MK at any height near the centre of a coronal hole. Wind acceleration by temperature effects is, therefore, inadequate as an explanation of the high-speed solar wind, and it becomes essential to look for other effects, involving the momentum and the energy of Alfvén waves.

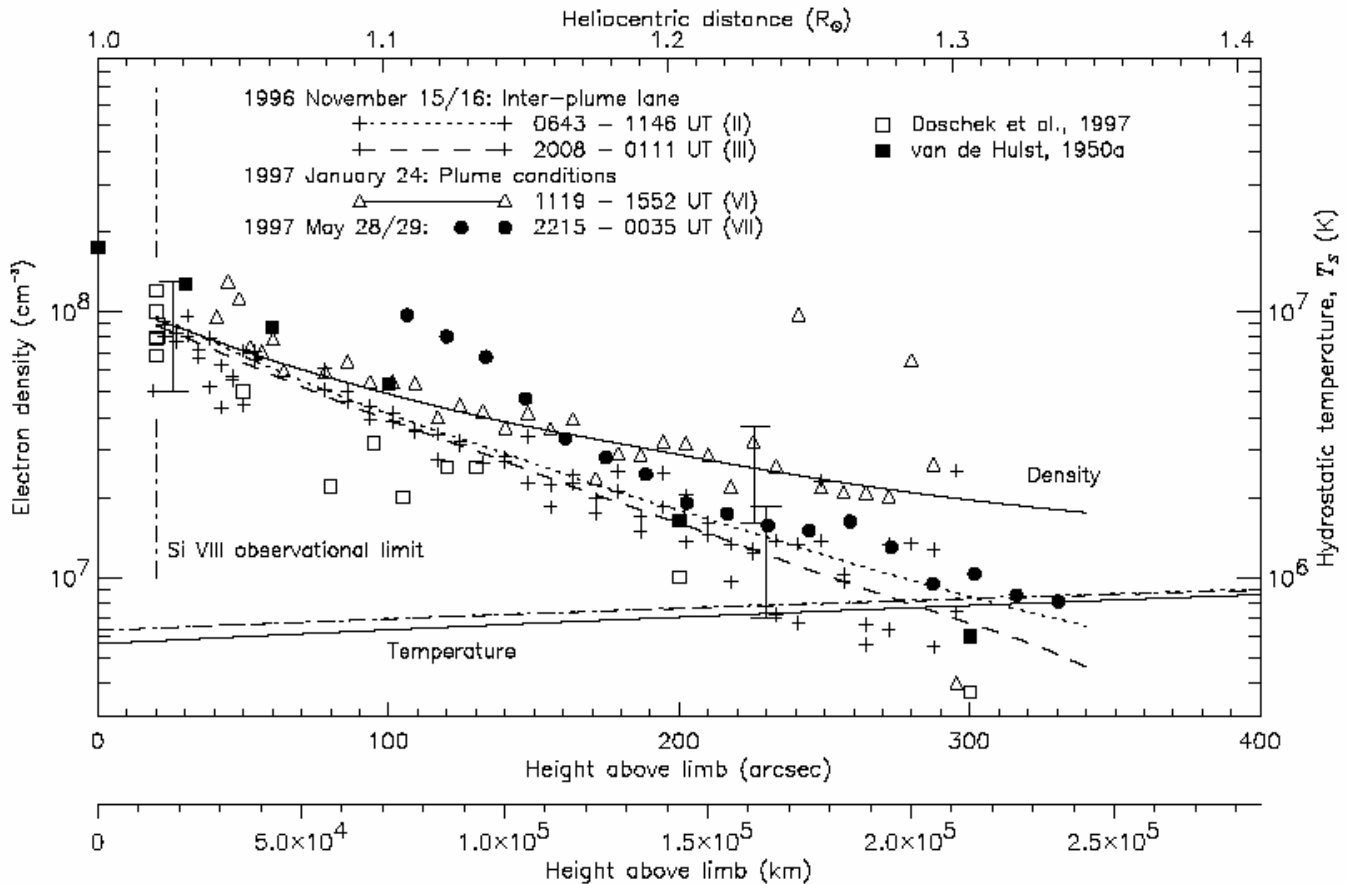


Fig. 4a. Electron densities derived from Si VIII line ratios and a comparison with the data in the literature. The hydrostatic temperature, T_s , used for the fits of the line Si VIII 144.5 nm (1445 Å) is plotted in the lower portion of the diagram, with a scale on the right-hand side. The points labeled "1997 May 28/29" are obtained from the ratios observed west of the polar plume assembly in a very dark region of the corona. The error bars indicate a density variation resulting from a $\pm 30\%$ uncertainty in the line ratio determination. Note that there is a small (3%) seasonal variation between the angular and the spatial scales for

different data sets. (From Wilhelm, Marsch, Dwivedi et al., 1998).

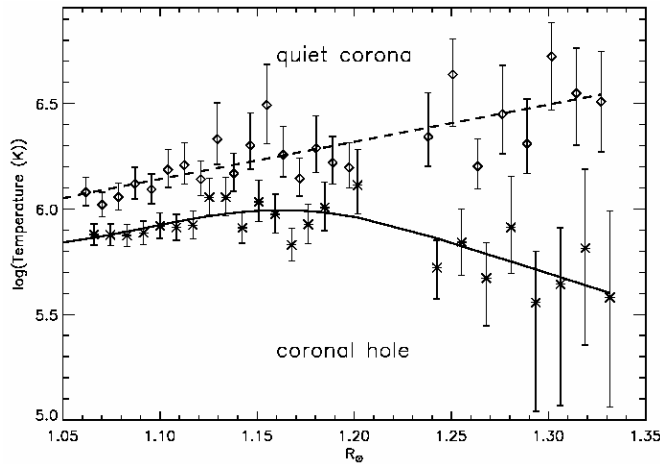


Fig. 4b. Temperature gradient measurement in the quiet corona (equatorial west limb) and the north polar coronal hole. (From David, Gabriel, Bely-Dubau, Fludra, Lamaire and Wilhelm, 1998). Observations were carried out on 21 May 1996, measured with the CDS and SUMER instruments on SOHO.

Recently we investigated the potential for plasma diagnostics of forbidden transitions from the ground levels in the nitrogen-like ions : Al VII, Si VIII, P IX, S X, Ar XII, K XIII and Ca XIV (Mohan, Landi and Dwivedi, 2003). We also studied the lines emitted by $n = 3$ levels of Si VIII. Figs. 5 and 6 respectively show the $(^4S_{3/2-2}P_{3/2})/(^4S_{3/2-2}P_{1/2})$ and $(^4S_{3/2-2}D_{3/2})/(^4S_{3/2-2}D_{5/2})$ line intensity ratios, which can be effectively used for density diagnostics in the solar corona. Some of the lines have been measured by SUMER for the first time. We investigated the effects of photospheric radiation, proton collisional excitations, additional configurations and resonances on level populations, in order to assess the importance of these processes in the calculation of line emissivities. We compared the line ratios with observations from SUMER on quiet-Sun and active regions and measured the electron density and temperature of the emitting plasma. We showed that in few cases current atomic data are still not able to reproduce the observations and that further work is required to solve inconsistencies between observations and theoretical predictions. We have also investigated FIP effect measurements in the off-limb corona (Dwivedi, Curdt and Wilhelm, 1999; Dwivedi, Mohan and Landi, 2003). We found that Mg/Ne relative abundance is highly variable in the complex, cool core of the active region, strongly correlated with line intensity and magnetic structures. Mg abundance enhancements relative to Ne reach up to a factor of 8.8. In off-limb active region plasma the FIP bias inside elements' class is dependent on the FIP value, being higher for the very low-FIP element K. The FIP bias versus FIP problem is still open.

Line shifts and broadenings give information about the dynamic nature of the solar and stellar atmospheres. The transition region spectra from the solar atmosphere are characterized by broadened line profiles. The nature of this excess broadening puts constraints on possible heating

processes. Systematic red shifts in transition region lines have

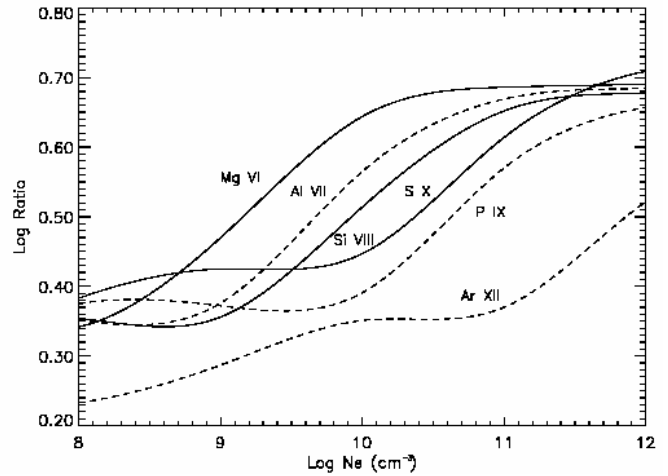


Fig. 5. Line intensity ratio involving the ground forbidden transitions $(^4S_{3/2-2}P_{3/2})/(^4S_{3/2-2}P_{1/2})$ as a function of the electron density, along the N-like sequence. (From Mohan, Landi and Dwivedi, 2003).

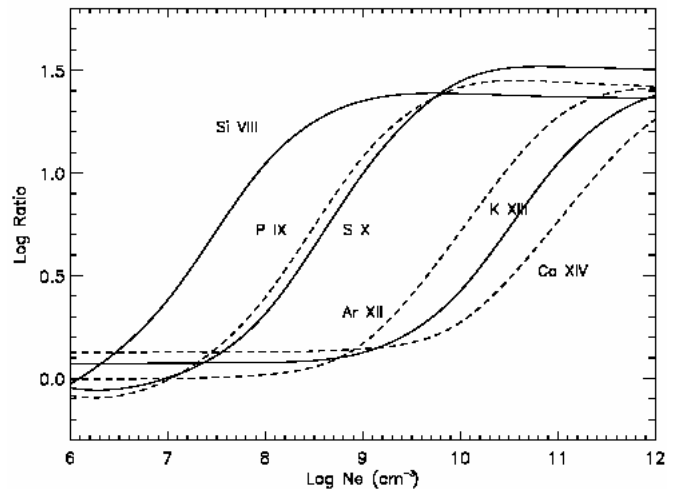


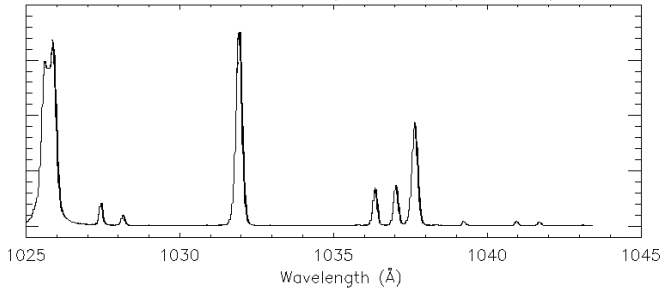
Fig. 6. Line intensity ratio involving the ground forbidden transitions $(^4S_{3/2-2}D_{3/2})/(^4S_{3/2-2}D_{5/2})$ as a function of the electron density, along the N-like sequence. (From Mohan, Landi and Dwivedi, 2003).

been observed in both solar and stellar spectra of late-type stars. On the Sun, outflows of coronal material have been correlated with coronal holes. The excess broadening of coronal lines above the limb provides information on wave propagation in the solar wind. Striking difference in the width of line profiles observed on disk and in a polar coronal hole (cf., Fig. 7) led to the discovery of the large velocity anisotropy, and solar wind acceleration by ion-cyclotron resonance (Kohl, Noci, Antonucci et al., 1997). An intriguing observation with the UVCS has shown that particular ions, specifically highly ionized oxygen atoms, have temperatures in coronal holes, some 100 MK, that are much higher than those characterized by electrons and protons making up the bulk of the plasma (Kohl, Noci, Antonucci et al., 1997). There seems to be some directionality to the oxygen temperatures --- they are higher perpendicular to the

magnetic field lines than parallel to them, a result that is in agreement with interplanetary spacecraft sampling the particles making up the solar wind. The observation seems to call for high-frequency ion-cyclotron waves (Tu, Marsch, Wilhelm and Curdt, 1998) that are produced lower down in the atmosphere as low-frequency waves but which through some cascade process end up at the observed frequencies.

O VI $\lambda\lambda$ 1032, 1037 line widths

SOLAR DISK (SUMER/SOHO)



N. Pole, 2.1 R_{\odot} (UVCS/SOHO)

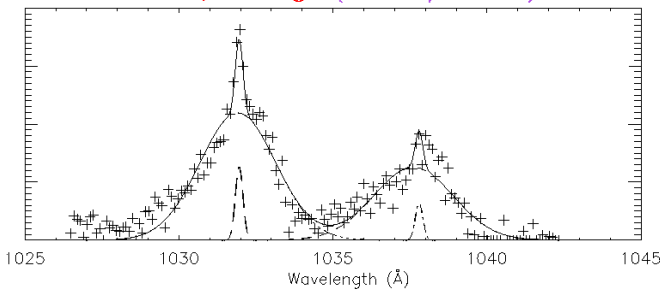


Fig. 7. This image shows UVCS/SOHO observations of the O VI 103.2 nm (1032 Å) and 103.7 nm (1037 Å) line profiles at 2.1 solar radii, in a polar coronal hole (lower panel) (Kohl, Noci, Antonucci et al., 1997). Each line consists of the coronal profile and narrow contribution from stray light plus F corona, which are separately constrained. The data points are shown as crosses, coronal profiles by dashes, and the total observed profile by a solid line. The widths of the coronal emission lines tell us about the ion velocity distribution measured along the line of sight. These extremely broad O VI lines yield velocities up to 500 km s⁻¹, which corresponds to kinetic temperatures of 200 MK. For comparison the SUMER/UVCS solar disk observations in the same range of spectrum (upper panel) are shown. The respective O VI 103.2 nm and 103.7 nm lines are much narrower, with widths of about 30 km s⁻¹. (Credit: UVCS, SUMER, ESA-NASA).

3. Coronal holes and the solar wind

Observations from the Skylab firmly established that the high-speed solar wind originates in coronal holes which are well-defined regions of strongly-reduced ultraviolet and X-ray emissions (Zirker 1977). More recent data from Ulysses show the importance of the polar coronal holes, particularly at times near the solar minimum, when dipole field dominates the magnetic field configuration of the Sun. The mechanism for accelerating the wind to the high values observed, of the order of 800 km s⁻¹, is not yet fully understood. The Parker model is based on a thermally-driven wind. To reach such high velocities, temperatures of the order 3 to 4 MK would be required near the base of the corona. However, other processes are available for acceleration of the wind, for example, the direct transfer of momentum from MHD waves,

with or without dissipation. This process results from the decrease of momentum of the waves as they enter less dense regions, coupled with the need to conserve momentum of the total system. If this transfer predominates, it may not be necessary to invoke very high coronal temperatures at the base of the corona. That the solar wind is emanating from coronal holes (open magnetic field regions in the corona) has been widely accepted since the Skylab era. But there was little additional direct observational evidence to support this view. Hassler, Dammasch, Lemaire et al. (1999) found the Ne VIII emission line blue shifted in the north polar coronal hole along the magnetic network boundary interfaces compared to the average quiet-Sun flow (cf., Fig. 8). These Ne VIII observations have revealed the first two-dimensional coronal images showing velocity structure in a coronal hole, and provided a strong evidence that coronal holes are indeed the source of the fast solar wind.

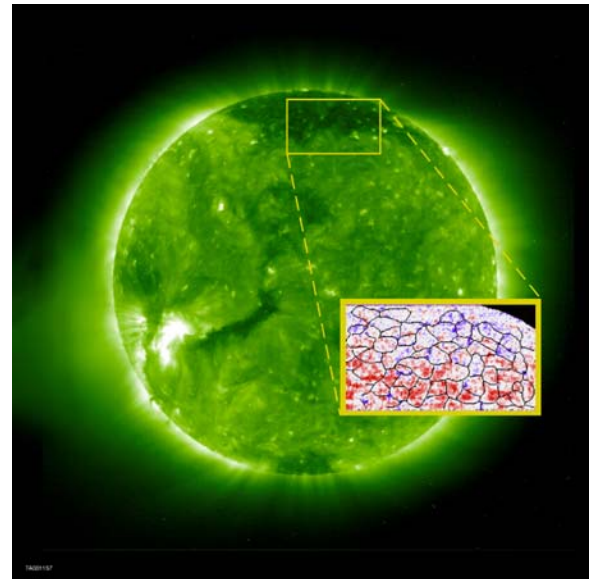


Fig. 8. The Solar corona and polar coronal holes observed from EIT and SUMER instruments on SOHO. The “zoomed-in” or “close-up” region in the image shows a Doppler velocity map of million degree gas at the base of the corona where the solar wind originates. Blue represents blue shifts or outflows and red represents red shifts or downflows. The blue regions are inside a coronal hole or open magnetic field region, where the high-speed solar wind is accelerated. Superposed are the edges of “honeycomb”-shaped patterns of magnetic fields at the surface of the Sun, where the strongest flows (dark blue) occur. (Credit : Don Hassler and SUMER-EIT/SOHO).

Tu, Zhou, Marsch et al. (2005) have now successfully identified the magnetic structures in the solar corona where the fast solar wind originates. Using images and Doppler maps from the SUMER spectrograph and magnetograms from the MDI instrument on the SOHO spacecraft, they have reported the solar wind flowing from funnel-shaped magnetic fields which are anchored in the lanes of the magnetic network near the surface of the Sun (cf., Fig. 9). This landmark research leads to a better understanding of the magnetic nature of the solar wind source region. The heavy ions in the coronal source regions emit radiation at certain ultraviolet wavelengths. When they flow towards Earth, the

wavelengths of the ultraviolet emission become shorter which can be used to identify the beginning of the solar wind outflow.

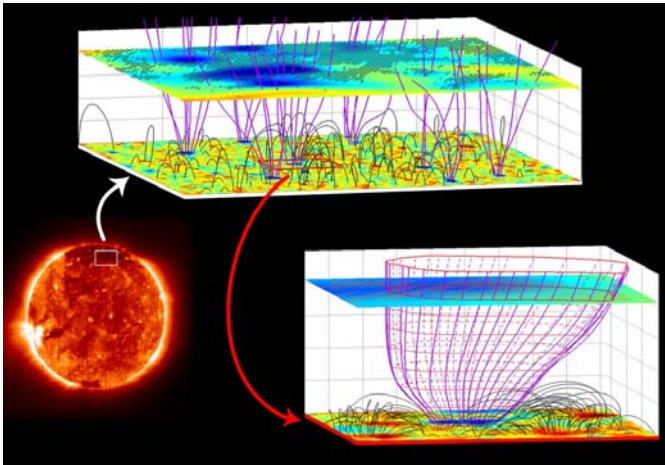


Fig. 9. This picture was constructed from measurements which were made on 21 September, 1996 on SOHO with the SUMER for Doppler spectroscopy of the coronal plasma, with the MDI for magnetograms of the Sun's surface, and the EIT for the context image of the Sun. The figure illustrates location and geometry of three-dimensional magnetic field structures in the solar atmosphere. The magenta coloured curves illustrate open field lines, and the dark gray solid arches show closed ones. In the lower plane, the magnetic field vertical component obtained at the photosphere by MDI is shown. In the upper plane, inserted at 20 600 km, the Ne VIII Doppler shift is compared with the model field. The shaded area indicates where the outflow speed of highly charged neon ions is larger than 7 km s^{-1} . The scale of the figure is significantly stretched in the vertical direction. The smaller figure in the lower right corner shows a single magnetic funnel, with the same scale in both vertical and horizontal directions. (Credit: SUMER, ESA/NASA)

Previously it was believed that the fast solar wind originates on any given open field line in the ionization layer of the hydrogen atom slightly above the photosphere. However, the low Doppler shift of an emission line from carbon ions shows that bulk outflow has not yet occurred at a height of 5,000 km. The solar wind plasma is now considered to be supplied by plasma stemming from the many small magnetic loops, with only a few thousand kilometers in height, crowding the funnel. Through magnetic reconnection plasma is fed from all the sides to the funnel, where it may be accelerated and finally form the solar wind. The fast solar wind starts to flow out from the top of funnels in coronal holes with a flow speed of about 10 km s^{-1} . This outflow is seen as large patches in Doppler blue shift (hatched areas in the Fig. 9) of a spectral line emitted by Ne^{+7} ions at a temperature of $600,000^\circ \text{ K}$, which can be used as a good tracer for the hot plasma flow. Through a comparison with the magnetic field, as extrapolated from the photosphere by means of the MDI magnetic data, it has been found that the blue-shift pattern of this line correlates best with the open field structures at 20,000 km.

Magnetic fields channel the transport of charged particles. Thus solar wind particles flow along invisible magnetic field lines much like cars on a highway. When the magnetic field lines bend straight out into space (as in coronal hole regions),

the solar wind acts like cars on a drag strip, racing along at high speed. When the magnetic field lines bend sharply back to the solar surface, like the pattern of iron filings around a bar magnet, the solar wind acts like cars in city traffic and emerges relatively slowly. This is well known for over three decades and is used to give a crude estimate for the speed of the solar wind – either fast or slow. In the new work by McIntosh and Leamon (2005), the speed and composition of the solar wind emerging from a given area of the solar corona are estimated from the characteristics of the chromosphere underlying that piece of corona. Using SOHO's EIT instrument as a "finder", they isolated regions of the solar corona with open magnetic field lines (coronal holes) and closed fields (active regions). Then, using the earth-orbiting TRACE to measure the time sound waves took to travel between the heights of formation of two chromospheric continua, they were able to demonstrate that sound travel time predicted not only solar wind speed measured by ACE but its isotopic composition as well.

4. Wave activity

Hassler et al. (1990) carried out a rocket-borne experiment to observe off-limb line width profile of Mg X 60.9 nm (609 \AA) and 62.5 nm (625 \AA) and reported the increasing line width with altitude (up to 70,000 km). This observation provided the first signature of outward propagating undamped Alfvén waves. SUMER and CDS spectrometers recorded several line profiles and found the broadening of emission lines. These results are consistent with outward propagation of undamped Alfvén waves travelling through regions of decreasing density (Erdélyi, Doyle, Perez and Wilhelm, 1998). However, Harrison, Hood and Pike (2002) reported the narrowing of the Mg X 62.5 nm (625 \AA) line with height in the quiet near-equatorial solar corona, and concluded that this narrowing is likely evidence of dissipation of Alfvén waves in closed field-line regions. Similarly, a significant change in slope of the line width as a function of height was seen in polar coronal holes by O'Shea, Banerjee and Poedts (2003) at an altitude of $\approx 65 \text{ Mm}$. These results obtained with the CDS, if confirmed, could be crucial in understanding the coronal heating mechanisms. Due to the broad instrumental profile, the CDS instrument can only study line-width variations and cannot provide measurements of the line-width itself, and, hence, of the effective ion temperature. Since the latter quantity is critical in constraining theoretical models of coronal heating and solar wind acceleration, for instance, through the dissipation of high-frequency waves generated by chromospheric reconnection, Wilhelm, Dwivedi and Teriaca (2004) studied the problem further by analysing data recorded with the SUMER spectrograph in the Mg X doublet together with other neighbouring lines in both the quiet equatorial corona and in a polar coronal hole. Due to the high spectral resolution of SUMER, they were able to obtain profiles of both Mg X emission lines and measure their widths and variations as a function of height. Their work

showed that line widths of both components of the Mg X doublet measured by SUMER monotonically increase in the low corona in equatorial regions in altitude ranges for which scattered radiation from the disk does not play a major rôle. They did not find any evidence for a narrowing of the emission lines

above 50 Mm. The same statement applies for a coronal hole, but they could not exclude the possibility of a constant width above 80 Mm (cf., Fig. 10).

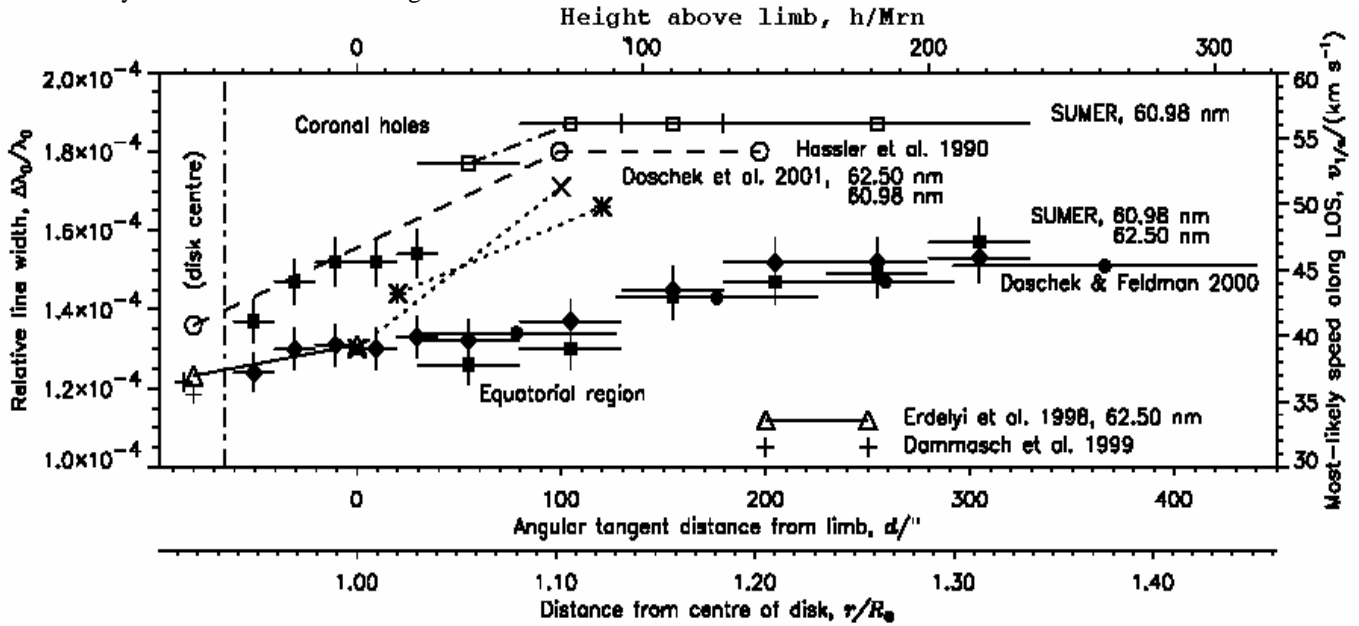


Fig. 10. Relative line-width variations as a function of radial distance from the Sun. Literature data and results obtained in this work (annotated "SUMER") are compiled for the Mg X doublet in equatorial and coronal hole regions. A classification of the Hassler et al. observations, of which only three typical values are shown, is not defined in their 1990 paper. Integration intervals and the SUMER uncertainty margins are marked by horizontal and vertical bars. Related data points are in some cases connected by lines of various styles. They are meant to improve the orientation of the reader, but not as physical interpolations, in particular, for those points representative of centre-of-disk values displayed here near $-80''$. (From Wilhelm, Dwivedi and Teriaca, 2004).

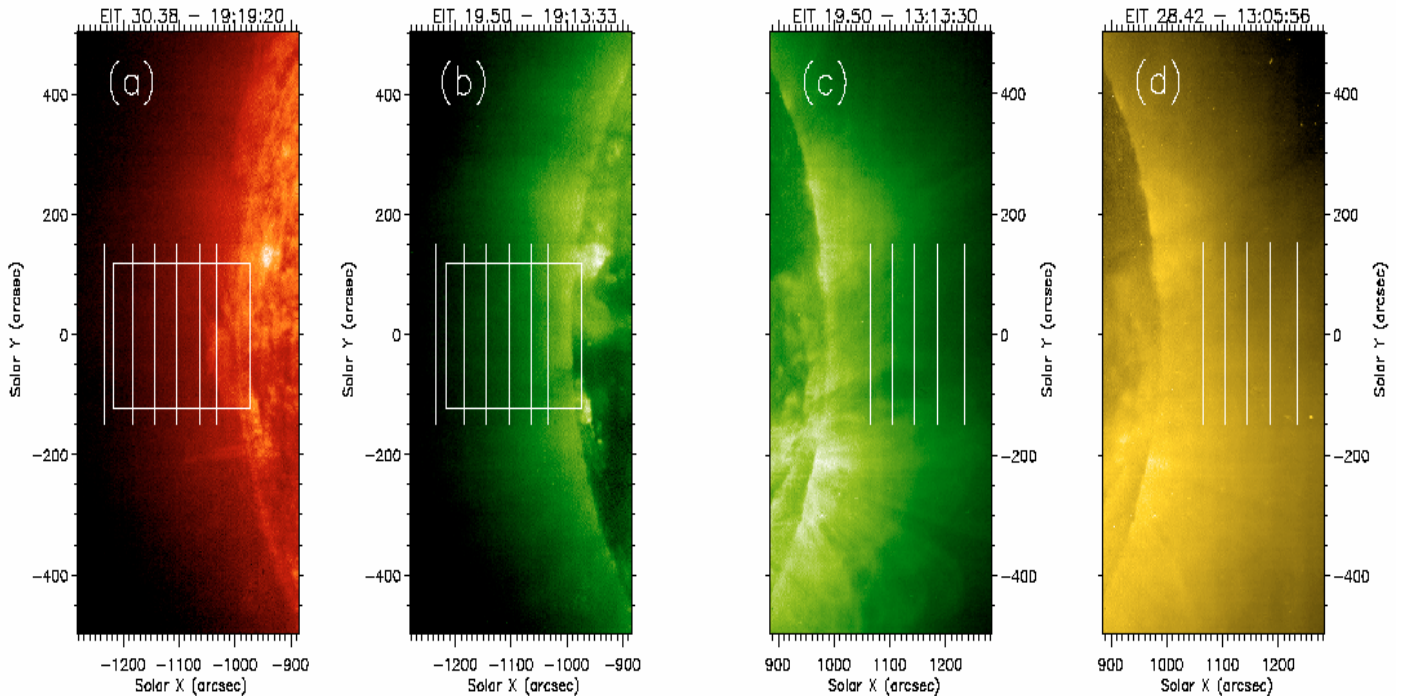


Fig. 11. Positions of the CDS FOVs (rectangles) and the SUMER slit pointing locations in relation to He II, Fe XII and Fe XV solar images of 4 December, 2003 (courtesy of the EIT consortium). Joint observations were obtained in the eastern corona. At low altitudes, a prominence caused a slight

disturbance there. (a) He II spectral window; and (b) Fe XII window near the east limb; (c) Fe XII window; and (d) Fe XV window near the west limb. (From Wilhelm, Fludra, Teriaca, Harrison, Dwivedi and Pike, 2005).

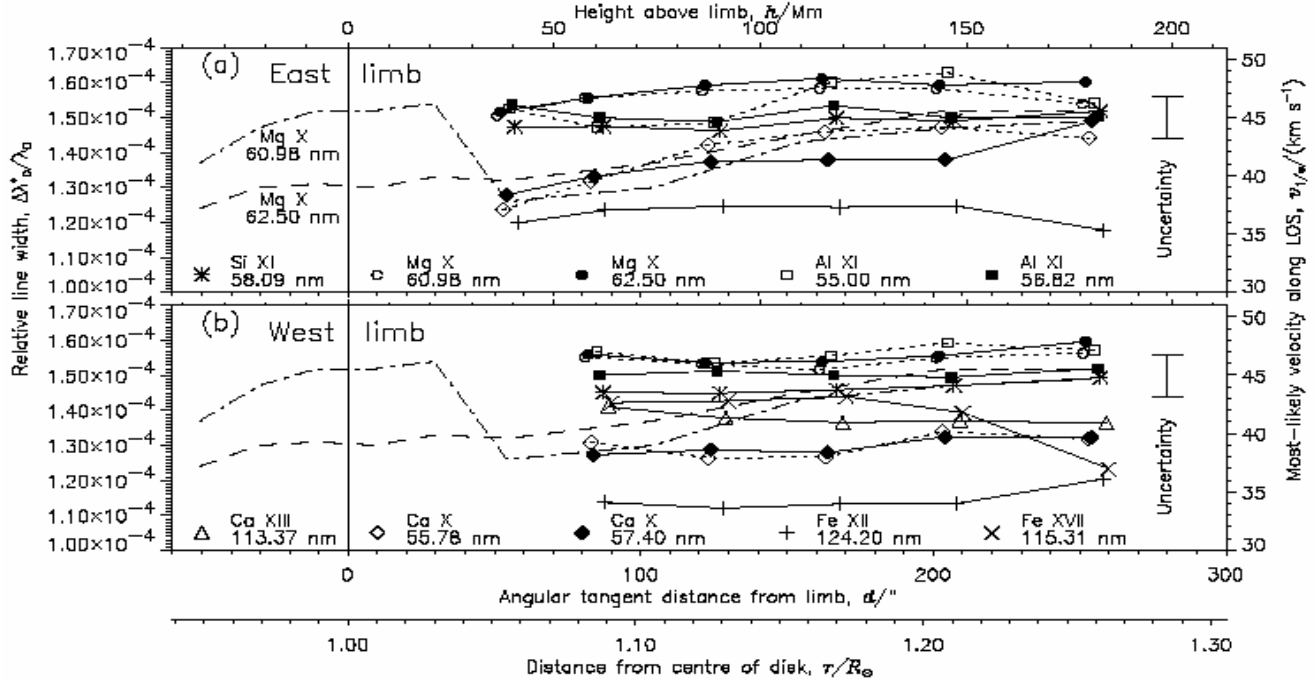


Fig. 12. Summary of the SUMER line-width measurements in terms of the relative line width, $\Delta\lambda_D^* / \lambda_0$, of the various ions, as well as their most-likely velocity along the LOS, $v_{l/e}$, as a function of distance from the limb. (a) Measurements above the east limb; (b) above west limb. The dashed and dash-dotted lines indicate the Mg X observations of SUMER in November 1996. The increase of the width of the 60.98 nm line near the limb is caused by blends of O III and O IV transition-region lines (cf., Wilhelm, Dwivedi and Teriaca, 2004). Near the centre of the solar disk a value of $\Delta\lambda_D^* / \lambda_0 \approx 1.2 \times 10^{-4}$ was observed for Mg X (Erdélyi, Doyle, Perez and Wilhelm, 1998; Dammasch, Hassler, Wilhelm and Curdt, 1999). At each slit position, an altitude range of $\approx 10''$ was covered. For the sake of clarity, the plot symbols of the various spectral lines are spread over this range. (From Wilhelm, Fludra, Teriaca, Harrison, Dwivedi and Pike, 2005).

While there have been reports of emission-line broadening with altitude, using SUMER, the CDS observations presented by Harrison, Hood and Pike (2002), already noted, appeared to show emission-line narrowing. In order to resolve the apparent discrepancies, a joint CDS/SUMER observational sequence was successfully executed during the SOHO/MEDOC campaign in November and December 2003. The joint measurements were performed near the east limb (cf., Wilhelm, Fludra, Teriaca, Harrison, Dwivedi and Pike, 2005). The pointing locations of the spectrometers are shown in Figs. 11a and 11b superimposed on He II and Fe XII solar images taken by EIT. In the western corona, SUMER made additional exposures with a similar observational sequence from 13:02 to 15:06 UTC. Since the corona was very hot there, the slit positions are shown together with the Fe XII and Fe XV windows of EIT in Figs. 11c and 11d.

The relative widths of the spectral lines observed by SUMER are shown in Fig. 12, separately for the eastern and western FOVs. In cases for which more than one observation was available, mean values have been shown. The range of $v_{l/e}$ extends from 35 km s^{-1} to 49 km s^{-1} in the relatively quiet eastern corona, and from 33 km s^{-1} to 48 km s^{-1} in the active western corona. No significant differences could be noticed within the uncertainty margins. The Mg X and Ca X lines show slight increases with height in the east, but are rather constant in the west. The Fe XII line is a little narrower in the

west. Of particular interest was that the lines of Ca XIII and Fe XVIII were seen in the west, where they could be compared with the Ca X and Fe XII lines along the same LOS. In the relatively quiet equatorial corona above a small prominence, Wilhelm, Fludra, Teriaca, Harrison, Dwivedi and Pike (2005) found none or very slight increase of the line widths of coronal emission lines with altitude from measurements both with CDS and SUMER. Taking the combined uncertainty margins into account, the relative variations for Mg X were considered to be consistent, although the absolute widths could not be compared given the different instrumental spectral transfer functions. The SUMER observations indicated even less line-width variations with height in the more active corona. Singh, Ichimoto, Sakurai and Muneer (2003) found height variations of line profiles in the visible light that depended on the formation temperatures of the lines. So, the solar conditions appear to have a direct influence on the line-width variations with height. Whether this dependence can account for the past apparent discrepancies cannot unambiguously be decided with the information available. More observations for different coronal activity levels are needed for this task. However, this joint study concluded that CDS and SUMER relative line-width measurements did not lead to inconsistencies if the same solar region is under study.

Dwivedi and Srivastava (2006) have investigated the effect of viscosity and magnetic diffusivity on the spatial variation of damping length scales and energy flux density of high

frequency Alfvén waves as a function of radial height, and have concluded a strong viscous and resistive damping of Alfvén waves in coronal holes. This result is in agreement with O'Shea, Banerjee and Doyle (2005) who find the decrease in the line widths above a radial height of about $1.23 R_{\odot}$ and attribute it to a reduction in the non-thermal component of the line widths caused by a damping of upwardly propagating Alfvén waves.

5. Concluding remarks

A large amount of information concerning the physical processes, taking place in the solar atmosphere has been made available in recent years from highly successful spacecraft SOHO, and TRACE. We have presented only a few of the significant results, mainly from the SUMER/SOHO spectrograph, which speak of a tremendous progress made in pinpointing the processes that maintain the Sun's hot corona and accelerate the solar wind as well as its source region. And the quest to unlock the Sun's mysteries goes on...

Acknowledgements. I would like to thank K. Wilhelm for critical reading of the manuscript, and for valuable comments. This work is supported by the Indian Space Research Organization (ISRO) under its RESPOND programme.

References

- W. A. Baum, F. S. Johnson, J. J. Oberly, C. C. Rockwood, C. V. Strain and R. Tousey, "Solar ultraviolet spectrum to 88 kilometers," *Phys. Rev.*, vol. 70, pp. 781-782, 1946.
- J. C. Brown, B. N. Dwivedi, Y. M. Almléaky and P. A. Sweet, "The interpretation of density sensitive line diagnostics from inhomogeneous plasmas. II - Non-isothermal plasmas," *Astron. Astrophys.*, vol. 249, pp. 277-283, 1991.
- W. Curdt, P. Brekke, U. Feldman, K. Wilhelm, B. N. Dwivedi, U. Schühle and P. Lemaire, "The SUMER spectral atlas of solar-disk features," *Astron. Astrophys.*, vol. 375, pp. 591-613, 2001.
- I. E. Dammasch, D. M. Hassler, K. Wilhelm and W. Curdt, "Solar Mg X and Fe XII wavelengths measured by SUMER," in *Proc. of 8th SOHO workshop: Plasma dynamics and diagnostics in the solar transition region and corona*, ESA SP - 446, 1999, pp. 263 - 268.
- C. David, A. H. Gabriel, F. Bely-Dubau, A. Fludra, P. Lemaire and K. Wilhelm, "Measurement of the electron temperature gradient in a solar coronal hole," *Astron. Astrophys.*, vol. 336, pp. L90 - L94, 1998.
- B. N. Dwivedi, "EUV spectroscopy as a plasma diagnostic," *Space Sci. Rev.*, vol. 65, pp. 289-316, 1994.
- B. N. Dwivedi, (Ed.), *Dynamic Sun*, Cambridge University Press, 2003.
- B. N. Dwivedi, "Our ultraviolet Sun," *Current Science*, vol. 91, pp. 587-595, 2006.
- B. N. Dwivedi, W. Curdt and K. Wilhelm, "Analysis of EUV off-limb spectra obtained with SUMER/SOHO: Ne VI/Mg VI emission lines," *Astrophys. J.*, vol. 517, pp. 516-525, 1999.
- B. N. Dwivedi and A. Mohan, "SOHO hunts elusive solar prey," *Current Science*, vol. 72, pp. 437-440, 1997.
- B. N. Dwivedi, A. Mohan and E. Landi, "FIP effect and FIP-dependent bias in the solar corona," in *Stars as Suns : activity, evolution and planets*, A. K. Dupree and A. O. Benz, Eds. ASP Conf. Ser., vol. 219, pp. 493-497, 2003.
- B. N. Dwivedi, A. Mohan and K. Wilhelm, "Vacuum-ultraviolet emission line diagnostics for solar plasma," in *Dynamic Sun*, B. N. Dwivedi, Ed. Cambridge University Press, 2003, pp. 353-373.
- B. N. Dwivedi and K. J. H. Phillips, "The Paradox of the Sun's hot corona," in *The Scientific American Special Edition "New Light on the Solar System"*, October 2003, pp. 4-11 (updated from the *Scientific American* June 2001 issue).
- B. N. Dwivedi and A. K. Srivastava, "On the propagation and dissipation of Alfvén waves in coronal holes," *Solar Physics*, vol. 237, pp. 143-152, 2006.
- B. Edlén, "Die deutung der emissionslinien in spektrum der sonnenkorona," *Zeitschrift für Astrophysik*, vol. 22, pp. 30 - 64, 1943.
- R. Erdélyi, J. G. Doyle, M. E. Perez and K. Wilhelm, "Center-to-limb line width measurements of solar chromospheric, transition region and coronal lines," *Astron. Astrophys.*, vol. 337, pp. 287-293, 1998.
- R. A. Harrison, A. W. Hood and C. D. Pike, "Off-limb EUV line profiles and the search for wave activity in the low corona," *Astron. Astrophys.*, vol. 392, pp. 319-327, 2003.
- D. M. Hassler, G. J. Rottman, E. C. Shoub and T. E. Holzer, "Line broadening of Mg X 609 and 625 Å coronal emission lines observed above the solar limb," *Astrophys. J.*, vol. 348, pp. L77 - L80, 1990.
- D. M. Hassler et al., "Solar wind outflow and the chromospheric magnetic network," *Science*, vol. 283, pp. 810-813, 1999.
- J. L. Kohl et al., "First results from the SOHO ultraviolet coronagraph spectrometer," *Solar Phys.*, vol. 175, pp. 613-644, 1997.
- P. Lemaire et al., "First results of the SUMER telescope and spectrometer on SOHO - II. Imagery and data management," *Solar Phys.*, vol. 170, pp. 105-122, 1997.
- H. E. Mason and B. C. Monsignori-Fossi, "Spectroscopic diagnostics in the VUV for solar and stellar plasmas," *Astron. Astrophys. Rev.*, vol. 6, pp. 123-179, 1994.
- S. W. McIntosh, J. C. Brown and P. G. Judge, "The relation between line ratio and emission measure analyses," *Astron. Astrophys.*, vol. 333, pp. 333-337, 1998.
- S. W. McIntosh and R. J. Leamon, "Is there a chromospheric footprint of the solar wind?," *Astrophys. J.*, vol. 624, pp. L117-L120, 2005.
- A. Mohan, E. Landi and B. N. Dwivedi, "On the EUV/UV plasma diagnostics for nitrogen-like ions from spectra obtained by SOHO/SUMER," *Astrophys. J.*, vol. 582, pp. 1162-1171, 2003.
- E. O'Shea, D. Banerjee and J. G. Doyle, "On the widths and ratios of Mg X 609.79 and 624.94 Å lines in polar off-limb regions," *Astron. Astrophys.*, vol. 436, pp. L43-L46, 2005.
- E. O'Shea, D. Banerjee and S. Poedts, "Variation of coronal line widths on and off the disk," *Astron. Astrophys.*, vol. 400, pp. 1065-1070, 2003.
- J. Singh, K. Ichimoto, T. Sakurai and S. Muneer, "Spectroscopic studies of the solar corona. IV. physical properties of coronal structure," *Astrophys. J.*, vol. 585, pp. 516-523, 2003.
- C. -Y. Tu, W. Marsch, K. Wilhelm and W. Curdt, "Ion temperatures in a solar polar coronal hole observed by SUMER on SOHO," *Astrophys. J.*, vol. 503, pp. 475-488, 1998.
- C. -Y. Tu et al., "Solar wind origin in coronal funnels," *Science*, vol. 308, pp. 519-523, 2005.
- K. Wilhelm et al., "SUMER - Solar Ultraviolet Measurements of Emitted Radiation," *Solar Phys.*, vol. 162, pp. 189-231, 1995.
- K. Wilhelm et al., "First results of the SUMER telescope and spectrometer on SOHO - I. spectra and spectroradiometry," *Solar Phys.*, vol. 170, pp. 75-104, 1997.
- K. Wilhelm, B. N. Dwivedi, E. Marsch and U. Feldman, "Observations of the Sun at vacuum ultraviolet wavelengths from space. Part I : concepts and instrumentation," *Space Sci. Rev.*, vol. 111, pp. 415-480, 2004.
- K. Wilhelm, B. N. Dwivedi, E. Marsch and U. Feldman, *Space Sci. Rev.*, 2006, in preparation.
- K. Wilhelm, E. Marsch, B. N. Dwivedi, D. M. Hassler, P. Lemaire, A. H. Gabriel and M. C. E. Huber, "The solar corona above polar coronal holes as seen by SUMER on SOHO," *Astrophys. J.*, vol. 500, pp. 1023-1038, 1998.
- K. Wilhelm, B. N. Dwivedi and L. Teriaca, "On the widths of the Mg X lines near 60 nm in the corona," *Astron. Astrophys.*, vol. 415, pp. 1133-1139, 2004.
- K. Wilhelm, A. Fludra, L. Teriaca, R. A. Harrison, B. N. Dwivedi and C. D. Pike, "The widths of vacuum-ultraviolet spectral lines in the equatorial solar corona observed with CDS and SUMER," *Astron. Astrophys.*, vol. 435, pp. 733-741, 2005.
- J. B. Zirker, (ed.) *Coronal Holes and High Speed Solar Wind Streams*, Colorado Associated Univ. Press, Boulder, 1977.